Structural and Functional Heterogeneity among the Zinc Fingers of Human MRE-Binding Transcription Factor-1†

Xiaohua Chen, Anshu Agarwal, and David P. Giedroc*

Department of Biochemistry and Biophysics, Center for Macromolecular Design, Texas A&M University, College Station, Texas 77843-2128

Received April 15, 1998; Revised Manuscript Received June 11, 1998

ABSTRACT: MRE-binding transcription factor-1 (MTF-1) activates the expression of metallothionein (MT) genes in mouse and human cells upon binding to one or more tandem metal-response elements (MREs; 5′-ctnTGCRCnCgGCCc) in the MT promoter. MTF-1 contains six Cys_2-His_2 zinc finger sequences. Previous work suggests that the zinc finger domain itself may function as a zinc sensor in zinc-activated expression of MTs. To obtain molecular insight into MTF-1 function, a recombinant fragment of MTF-1 containing only the zinc finger domain (denoted MTF-zf) has been purified using nondenaturing conditions and characterized with respect to zinc-binding properties, secondary structure, and DNA-binding activity. Different preparations of MTF-zf, following an anaerobic dialysis to quantify Zn(II) and reduced cysteine (by DTNB reactivity) content, reveal Zn(II)/MTF-zf stoichiometries ranging from 3.3 to 5.5 g at Zn(II) and 11−13 reduced thiolates (12 expected). Far-UV CD spectra reveal indistinguishable secondary structural content in all preparations, i.e., enough to fold just *three* of six zinc fingers of MTF-zf. Removal of additional zinc from MTF-zf gives rise to an insoluble apoprotein. Complex formation between a $Zn_{5.5}$ MTF-zf and a coumarin-labeled MREd-containing oligonucleotide as monitored by changes in the anisotropy of the coumarin fluorescence gives a $K_{app} = 3.8\ (\pm 0.5) \times 10^8\ M^{-1}$ (pH 7.0, 0.20 M NaCl, 25 °C). Investigation of the salt type and concentration dependence of K_{app} suggests significant contributions from both cation and anion release upon complex formation. $Zn_{5.5}$ MTF-zf exhibits a large negative heat capacity of complex formation with MREd and can discriminate among DNA duplexes which have mutations deposited on either the TGCRC core or the C-rich side of the MREd. Air oxidation of $Zn_{5.5}$ MTF-zf results in the reversible conversion of 6 of the 12 Cys thiolates to 3 disulfide bonds; as expected, this has no effect on the secondary structure of MTF-zf, but results in ≈30-fold reduction in K_{app} to $\approx 1.2 \times 10^7\ M^{-1}$. In contrast, fully reduced $Zn_{3.5}$ MTF-zf binds to the MREd with an affinity and [NaCl] dependence largely indistinguishable from those of $Zn_{5.5}$ MTF-zf. The zinc fingers in MTF-zf are physically and functionally inequivalent. A subset (≈3−4) of zinc fingers plays a structural role in folding and high-affinity MREd binding, while one or more additional fingers have properties potentially consistent with a metalloregulatory role.

Metal-responsive control of the expression of genes involved in metal metabolism and metal homeostasis allows an organism to tightly regulate the free concentration of beneficial metal ions such as zinc, copper, and iron within an acceptable range, while efficiently removing nonbeneficial or toxic metals. The molecular circuitry of metalloregulation has been well-established in only a few cases, including, for example, the detoxification of mercury and arsenic in bacteria and the regulation of iron and copper homeostasis in mammalian cells and yeast, respectively (for a review, see ref *1*). Regulation by zinc has only recently begun to be understood (*2*−*5*).

Zinc finger proteins, zinc metalloproteins that are known to regulate gene expression, are excellent candidates for molecular sensors and/or transducers of altered intracellular concentrations of free zinc (*6*). New molecular insights into the participation of zinc finger proteins as zinc-responsive metalloregulatory proteins have been gleaned from studies on the induction of metallothionein (MT)[1] gene expression by heavy metals, including zinc and cadmium (*7*, *8*). Vertebrate MTs are low molecular weight, cysteine-rich polypeptides that bind many kinds of heavy metals, including Zn(II), Cd(II), Cu(II), and Co(II) (*9*). Targeted gene disruption experiments suggest that MT I and MT II are involved in many cellular processes including metal ion homeostasis, adaptation to oxidative stress, and metal detoxification (*10*, *11*). The synthesis of MTs in vertebrates is controlled at the transcriptional level and can be induced by a range of heavy metals including zinc, cadmium, mercury, and copper (*8*). This induction requires a cis-acting DNA element termed a metal response element (MRE) (*12*) and the Cys_2-His_2 zinc finger protein metalloregulatory or MRE-binding

† This work was supported by NIH Grant GM42569 and the Robert A. Welch Foundation (A-1295).

* To whom correspondence should be addressed. Telephone: 409-845-4231. FAX: 409-862-4718. E-mail: giedroc@bioch.tamu.edu.

[1] Abbreviations: DTNB, 5,5′-dithiobis(2-nitrobenzoic acid); DTT, dithiothreitol; MOPS, 3-(*N*-morpholino)propanesulfonic acid; MRE, metal-response element; MT, metallothionein; MTF-1, MRE-binding transcription factor-1.

S0006-2960(98)00843-5 CCC: $15.00
Published on Web 07/24/1998

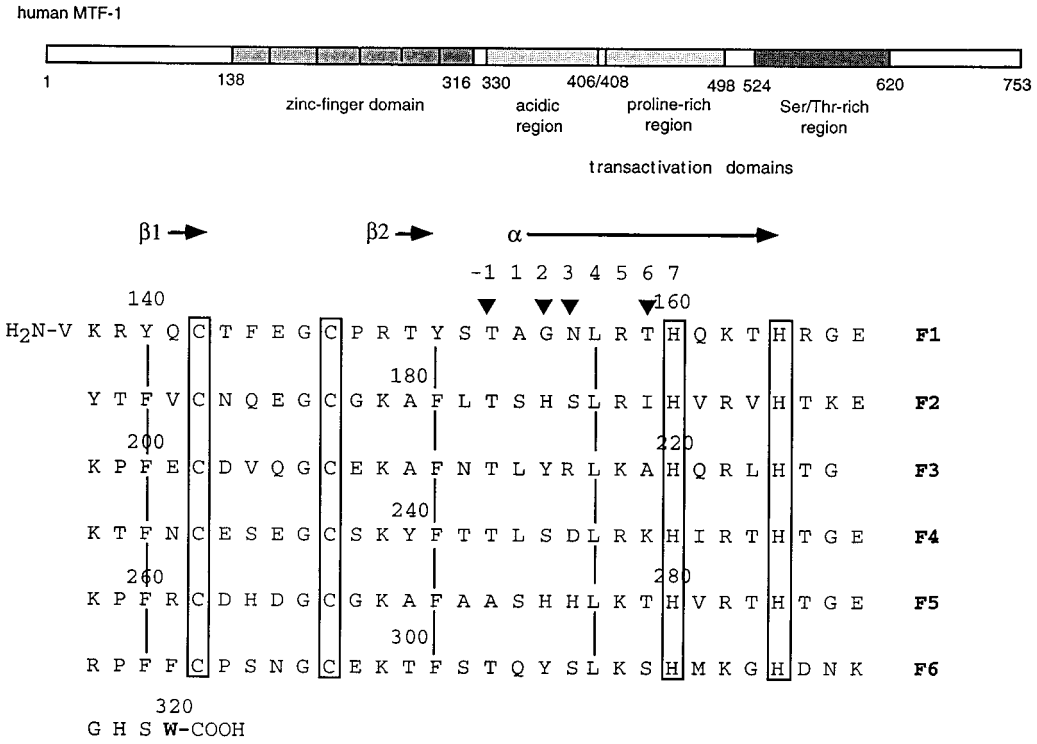

FIGURE 1: Primary structure representation and amino acid sequence of MTF-zf, the zinc finger domain region of human MTF-1 characterized in this study. Plausible specificity determinants at −1, +2, +3, and +6 are shown for each of the zinc fingers (▼).

transcription factor-1 (MTF-1) (*2*, *13*, *14*). Many MREs contain an overlapping binding site for the general transcription factor Sp1, which is also a Cys_2-His_2 zinc finger protein (*15*). MTF-1 has been proposed to play a metalloregulatory role in mammalian cells by directly sensing changes in intracellular zinc concentration and inducing MT expression (*3*, *13*, *16*); Sp1, on the other hand, is not similarly regulated (*3*, *17*). Gene knockout experiments in mice identify MTF-1 as an essential factor in both basal and zinc-dependent regulation of gene expression in mammalian cells (*14*).

MTF-1 encoded by human and mouse cells is a large protein consisting of multiple functional domains, including at least three distinct transactivation domains located in the C-terminal half of the molecule, and a six Cys_2-His_2 zinc finger domain within the N-terminal part of the molecule (Figure 1) (*16*). The Cys_2-His_2 zinc finger is a structurally well-defined DNA-binding motif (*18*); previous studies reveal that all or a subset of the zinc fingers are coincident with the MRE-binding domain (*3*).

Westin and Schaffner (*15*) proposed a simple metalloregulatory model in which constitutively expressed MTF-1, with an intrinsically low binding affinity for zinc, would bind Zn(II) only under conditions of zinc excess. All other zinc-requiring, but not zinc-*regulated*, factors (e.g., Sp1) would be saturated with zinc under all physiological conditions. Consistent with this idea is the finding that the N-terminal and zinc finger domains of human MTF-1 (residues 1−312), when fused to a general transcriptional activating domain (VP16), confer limited zinc responsiveness in vivo (*16*). A recent report shows that reversible activation of MRE binding by intact MTF-1 involves the interaction of Zn(II) with the zinc finger domain (*3*). This model is analogous to that proposed for the copper- and silver-dependent induction of MT expression in *S. cerevisiae* (*19*). Another attractive model invokes distinct classes of zinc finger domains in MTF-1 that differ in their intrinsic affinities for the metal as well as their functional role. In this model, a subset of zinc fingers might be structural sites that are always occupied with Zn(II) (higher affinity); these sites may be essential for MRE binding. Other zinc fingers in MTF-1 would play a regulatory role (lower affinity); they would become bound by Zn(II) (and perhaps other metal inducers of MT expression) as the intracellular concentration rises. The experiments described here present systematic studies directed toward obtaining molecular insight into the mechanism of MTF-1 action.

MATERIALS AND METHODS

Purification of MTF-zf. A bacterial expression plasmid, pT7mtf-zf, was constructed to express residues 137−320 of human MTF-1, denoted MTF-zf, by amplifying a DNA fragment via the polymerase chain reaction using the cDNA plasmid pChMTF-1 (kindly provided by Dr. Walter Schaffner, University of Zürich) as the template. The PCR primers incorporated *Nco*I and *Bgl*II restriction endonuclease sites, to permit subcloning of the crude PCR product directly into *Nco*I/*Bam*HI-restricted pET-3d (*20*). The 3′ PCR primer also directs substitution of the C-terminal Tyr^{320} of MTF-1 with Trp, which would become the only Trp in the molecule. Recombinant MTF-zf was inducibly expressed in *E. coli* BL21(DE3) transformed with pT7mtf-zf and pLysS to ampicillin and chloramphenicol resistance on Luria broth containing 100 μg/mL ampicillin and 17 μg/mL chloramphenicol at 15 °C (to increase the solubility of protein) to an $OD_{600} = 0.6$, and the cells were harvested. Frozen cells from 9 L of growth media were resuspended in lysis buffer (50 mM Tris-HCl, pH 8.0, 50 mM NaCl, 10 mM DTT, 50 μM $ZnSO_4$) and lysed by sonification. Polymin P [10% (w/v), pH 7.9] was added to the low-speed cellular supernatant to a final concentration of 0.2% to precipitate the nucleic

acids. The solution was centrifuged, and solid ammonium sulfate was added to the supernatant to a saturation of 55% on ice to precipitate MTF-zf and remove the PEI. The ammonium sulfate pellet was resuspended in MOPS buffer (50 mM MOPS, 0.20 M NaCl, 4 mM DTT, 50 μM $ZnSO_4$, pH 7.0), and dialyzed exhaustively against the same buffer to remove ammonium sulfate. The dialyzed fraction was applied to a Waters 600E HPLC system fitted with Poros QE-20 (1.7 mL) and Poros CM-20 (1.7 mL) columns connected in series equilibrated with the same MOPS buffer at 5.0 mL/min, and the columns were washed with 6 column volumes of the same buffer. MTF-zf, a basic protein, flows through the QE column, binds tightly to the CM column, and is eluted by applying a linear gradient of MOPS buffer to 2 M NaCl. MTF-zf elutes at ≈0.8 M NaCl and was collected. At this stage, MTF-zf is >90% homogeneous based on SDS−polyacrylamide gel analysis (data not shown). The identity of the this protein fraction as MTF-zf was confirmed by N-terminal sequencing (*N*-Val^{137}-Lys-Tyr-Gln-X-Thr-Phe-Glu-Gly-X-Pro-Arg-Thr; X is Cys), amino acid analysis, and MALDI-TOF mass spectrometry (M_r = 21 163.2; expected M_r = 21 166.8). Also, all preparations of MTF-zf exhibited fluorescence excitation (λ_{em} = 347 nm) and emission (λ_{ex} = 296 nm) spectra essentially indistinguishable from that of *N*-acetyltryptophanamide, showing that all preparations of MTF-zf contained the C-terminal Trp^{320}. Various aliquots of this material were subjected to exhaustive dialysis in an anaerobic glovebox (Vacuum-Atmospheres, Inc.) against metal-free buffer at pH 7.0, and the zinc content and number of reduced cysteines were determined by flame atomic absorption and DTNB reactivity anaerobically, respectively, using ϵ_{280} = 16 400 M^{-1} cm^{-1}, essentially as described (*21*).

Preparation of Coumarin-Labeled DNAs. Crude oligonucleotides (Operon Technologies) were resuspended in TE, purified by denaturing PAGE, electroeluted (S&S), loaded onto C18-cartridge (Alltech), eluted with 50% methanol, and evaporated to dryness. The 5′-hexylamine-linked oligonucleotides were reacted with a 30-fold excess of the fluorescent probe 7-diethylaminocoumarin-3-carboxylic acid, succinimidyl ester (Molecular Probes), at pH 8.5, room temperature in 40% DMF overnight. The solution was loaded onto a 5 mL Sephadex G-25 (Sigma) spun column to remove most of the unreacted probe, and then loaded onto a C4 Vydac HPLC column equilibrated with 0.1 M triethylamine acetate (TEA), pH 6.5, developed with an acetonitrile gradient (0.1 M TEA, pH 6.5, in CH_3CN). The pooled fraction was loaded onto a second C18-cartridge, eluted with 100% methanol, and evaporated to dryness. To prepare the duplexes shown in Figure 2, the purified coumarin-labeled oligonucleotides were annealed to their complementary unlabeled strands (1.05:1 unlabeled to labeled strand) at 95 °C for 5 min in 10 mM Tris-HCl, pH 7.5, followed by slow cooling to room temperature.

Fluorescence Measurements. All fluorescence polarization binding experiments were carried out with an SLM 8000 or 4800 spectrofluorometer operating in the steady-state mode fitted with Glan-Thompson polarizers used in the L format. The binding of MTF-zf to DNA was followed by monitoring the change in the apparent fluorescence anisotropy of the DNA. The excitation wavelength was 430 nm (4 mm slit width) with the total polarized emission intensity collected

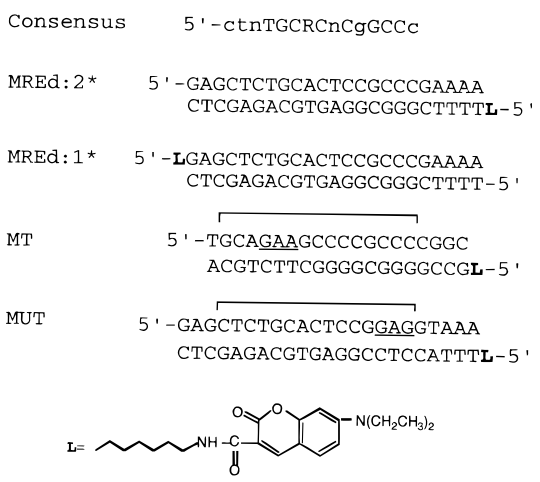

FIGURE 2: Sequences of the DNA duplexes used in this study. The nucleotides underlined in the MT and MUT oligonucleotides represent nonconservative substitutions within the currently defined consensus sequence. MT contains a binding site for the general transcription factor Sp1 (*26*) and diverges significantly from the consensus MRE sequence on the TGCRC side of the recognition element, while MUT contains nonconservative substitutions on the C-rich side of the element. The MUT sequence is nonfunctional in vivo (*15*).

with a Corning 3-71 cutoff filter. The polarization (*P*) and the anisotropy (r_{obs}) of the samples were calculated from

$$P = (I_{VV} - GI_{VH})/(I_{VV} + GI_{VH}) \quad (1)$$

$$r_{obs} = 2P/(3 - P) \quad (2)$$

where I_{VV} and I_{VH} are the intensities of the emitted light polarized parallel and perpendicular, respectively, to the incident vertically polarized excitation beam. The factor $G = I_{HV}/I_{HH}$ corrects the measured intensities for differences in the sensitivity of the detection of vertically and horizontally polarized emitted light ($G = 1.03 \pm 0.01$). Typically, 5−6 measurements of 10 s integration time each were collected and averaged to obtain I_{VV}, I_{VH}, I_{HV}, and I_{HH}. The corrected intensities were obtained after subtraction of background intensities measured with a buffer solution, and corrected for dilution. Total fluorescence intensity was 20-fold to 50-fold the background intensity of the buffer solution. Nonlinear least-squares fits to these binding isotherms to extract K_{app} and $r_{complex}$ were carried out assuming a 1:1 binding stoichiometry (consistent with stoichiometric titrations) (*22*) and a linear change in r_{obs} with fractional saturation of the DNA. The apparent total fluorescence emission intensity (*I*), calculated from $I = I_{VV} + 2I_{VH}$, is proportional to Q_i, the quantum yield of the free DNA (Q_o), and the saturated protein−DNA complex (Q_d). Depending on the oligonucleotide, Q_d/Q_o varied from 0.93 to 1.27, but appeared to differ somewhat from experiment to experiment. Isotherms (r_{obs} vs $[MTF\text{-}zf]_{total}$) converted to Θ vs $[MTF\text{-}zf]_{total}$ using $\Theta = (r_{obs} - r_o)/[(r_{complex} - r_{obs})(Q_d/Q_o) + r_{obs} - r_o]$ (*23*) returned K_{app} to within 30% of that obtained by fitting the r_{obs} vs $[MTF\text{-}zf]_{total}$ isotherms directly. Since this is well within the range of measurements obtained from replicate titrations, raw r_{obs} vs $[MTF\text{-}zf]_{total}$ isotherms were fit directly.

Circular Dichroism Spectroscopy. Far-UV CD spectra were collected on an AVIV 62DS spectropolarimeter operat-

Table 1: Analytical Properties of Various Preparations of MTF-zf[a]

preparation	treatment	Zn(II) content (g at mol^{-1})	reactive thiolates[e]
1	dialysis[b]	5.7 (±0.5)	12.2
2	dialysis[b]	3.3	11.7
3	dialysis[b]	4.7	ND[d]
4	dialysis[b]	5.5 (±0.5)	12.5
5	97 μM mag-fura-2 followed by dialysis[b]	3.5	12.5
6	dialysis[c]	5.0	12.5
7	98 μM mag-fura-2 followed by dialysis[c]	3.5	12.4

[a] MTF-zf preparations obtained as described under Materials and Methods with the exception of preparation 3 which was obtained via a denaturing purification strategy (R. Khan, A. Agarwal, and D. Giedroc, unpublished results). [MTF-zf] was obtained from $\epsilon_{280} = 16\,400$ M^{-1} cm^{-1}. [b] 4.2 molar equiv of the chelator; dialyzed anaerobically against 40 mM MOPS, 0.20 M NaCl, pH 7.0. [c] 4.2 molar equiv of the chelator; dialyzed anaerobically against 6 mM sodium phosphate, 0.20 M NaF, pH 7.0. [d] Not determined. [e] Determined by anaerobic reactivity with DTNB.

ing at 25.0 ± 0.1 °C in a 1 mm rectangular cell with an MTF-zf concentration of 6−7 μM in 6 mM sodium phosphate, pH 7.0, 0.20 M NaF. Identical spectra were obtained in 40 mM MOPS, pH 7.0, 0.20 M NaCl (data not shown). Typical acquisition parameters were 2 s time constant, 1 nm bandwidth, 4 replicates. All spectra were base-line-corrected by subtraction of an averaged scan derived from buffer, and are presented in units of mean residue ellipticity, $[\theta]_{MRE}$ (deg cm^2 dmol^{-1}).

RESULTS

Characterization of MTF-zf. The deduced primary structure of MTF-zf predicts the presence of six folded Cys_2-His_2-type zinc fingers (Figure 1). To test this prediction, a nondenaturing purification strategy was implemented to obtain reasonable quantities of highly purified MTF-zf (see Materials and Methods). All steps in the purification were done in air in the presence of reducing agent and at least 50 μM Zn(II) salts. The last step in the purification is an anaerobic dialysis against metal-free buffer, involving 3−5 changes over 8−17 h. These preparations were then subjected to Zn(II) atomic absorption and DTNB reactivity to quantify the number of free Cys in MTF-zf preparations. Analytical data for various preparations of MTF-zf prepared in this way are shown in Table 1. As can be seen, independent preparations of MTF-zf subjected to dialysis contain ≈3 to ≈6 g at Zn(II). All preparations contained approximately 12 reduced cysteines, consistent with predictions from the amino acid sequence. No preparation of MTF-zf prepared in this way contained less than ≈3 g at Zn(II).

The above data suggest that MTF-zf contains at least two classes of metal-binding sites based on equilibrium affinity; the bound Zn(II) from as many as three sites is readily lost upon dialysis, while that from the other three sites is not. To obtain further support for this, $Zn_{5.5}$ MTF-zf was treated with a slight excess of the chelator mag-fura-2 (*24*) (4.5 molar equiv) and subjected to a brief anaerobic dialysis. Mag-fura-2 has an affinity constant for Zn(II) under these solution conditions of 5×10^7 M^{-1} (*24*). An MTF-zf preparation obtained in this way contains 3.5 g at Zn(II) and 12 reduced thiolates (Table 1). This suggests that mag-fura-2 has a higher affinity for Zn(II) than the weak sites of MTF-zf; the tight Zn(II)-binding sites, on the contrary, have a significantly higher affinity than mag-fura-2 for Zn(II). Treatment of $Zn_{5.3}$ MTF-zf with a much stronger chelator, EDTA ($K_{Zn} \approx 10^{12}$ M^{-1}), strips all of the metal from MTF-zf to form an insoluble apoprotein under these conditions (data not shown). Treatment with an excess of methylmethanethiosulfonate to form apo *S*-methylated MTF-zf (*25*) also leads to the same result.

These experiments lead to the surprising finding that distinct preparations of MTF-zf can be obtained which contain from ≈3 to nearly 6 mol equiv of Zn(II). We next wished to determine the secondary structure content of each of these preparations using far-UV CD spectroscopy. This is a convenient assay to determine the extent of folded structure in each molecule. CD spectra are shown in Figure 3A,B for preparations of MTF-zf containing 3.5 or 5.5 g at Zn(II), as well as for $Zn_{3.5}$ MTF-1 to which excess Zn(II) was added. Surprisingly, each of these preparations is characterized by essentially identical $[\Theta]_{MRE}$ of a magnitude ($[\Theta]_{MRE}^{222} \approx -4300$ deg cm^2 dmol^{-1}) sufficient to fold approximately three zinc fingers of MTF-zf (*18*). Therefore, the three other putative zinc fingers of MTF-zf appear to bind Zn(II) very weakly at pH 7.0, in a way which does not induce significant α-helical structure. Interestingly, examination of the kinetics of air oxidation of the Cys thiolates in fully reduced $Zn_{5.5}$ MTF-zf reveals two distinct phases of reactivity which differ by a factor of ≈50, and possess amplitudes of approximately six thiolates each (Figure 3C). The simplest interpretation of this experiment is that the three weak binding Zn(II) sites do not readily protect the Cys thiolates from oxidation by molecular oxygen, in contrast with the three tight binding sites. As expected, this partial oxidation of MTF-zf has no effect on the secondary structure content of the molecule (Figure 3A).

DNA-Binding Activity of MTF-zf. It was next of interest to determine the extent to which various MTF-zf preparations bind to a 23 base pair coumarin-labeled oligonucleotide duplex harboring a single MREd consensus sequence (MREd:2*; cf. Figure 2). The stoichiometry of the interaction was determined directly to be 1:1, as expected (Figure 4). A representative MREd:2* binding isotherm obtained for $Zn_{5.5}$ MTF-zf at 0.20 M NaCl, 25 °C, pH 7.0, is shown in Figure 5A, with the solid curve the result of a nonlinear least-squares fit to a 1:1 binding model. Under these solution conditions, $K_{app} = 3.8\ (\pm 0.5) \times 10^8$ M^{-1} (Table 2). This is near the maximum magnitude of K_{app} that can be determined under these conditions. Two additional experiments were done to determine if the presence and/or position of the coumarin in the MREd:2* oligonucleotide has any effect on the binding affinity observed for MREd:2*. Binding isotherms were obtained with MREd:1* (Figure 2) under identical solution conditions (0.20 or 0.30 M NaCl, pH 7.0, 25 °C) with the results shown in Table 1. K_{app} for MREd:1* is indistinguishable from that of MREd:2* under both sets of solution

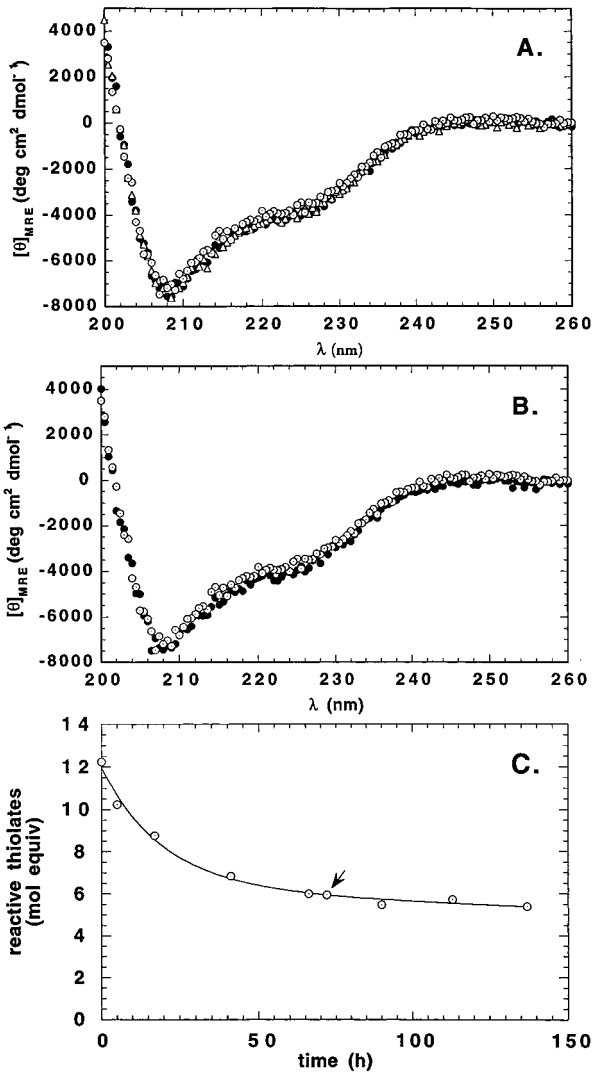

FIGURE 3: Far-UV CD spectra of various forms of MTF-zf. (A) $Zn_{5.5}$-Cys_{12} MTF-zf (●); $Zn_{(3)}$-Cys_6 MTF-zf (△); $Zn_{3.5}$-Cys_{12} MTF-zf (○). (B) $Zn_{3.5}$-Cys_{12} MTF-zf (○); $Zn_{3.5}$-Cys_{12} MTF-zf plus 55 μM $ZnCl_2$ (●). Conditions: 6 mM sodium phosphate, 0.20 M NaF, pH 7.0, 25 °C. (C) Time course of the oxidation of MTF-zf (5 μM) as monitored by the DTNB reaction. The solid line represents a double-exponential fit to the kinetic data: fast phase: 5.7 ± 0.8 thiolates, $k = 0.05$ h^{-1}; slow phase: 6.3 ± 0.8 thiolates; $k = 0.0011 \pm 0.0011$ h^{-1}. The arrow indicates the point at which MTF-zf was returned to an anaerobic atmosphere, to create $Zn_{(3)}$-Cys_6 MTF-zf.

conditions, although the total change in the anisotropy (Δr) is considerably smaller for MREd:1* [$\Delta r = 0.011$ (± 0.002)] relative to MREd:2* [$\Delta r = 0.036$ (± 0.005)]. Binding isotherms were also collected with MREd:2* in the presence of an excess concentration of unlabeled MREd duplex; nonlinear least-squares analysis of these isotherms returns a K_{app} for the unlabeled oligonucleotide essentially indistinguishable from either of the coumarin-labeled oligonucleotides (data not shown). These experiments show that MTF-zf binds to MREd:2* in a way which is not affected by the presence or the position of the coumarin and thus reflects the intrinsic properties of the MTF-zf−MREd interaction.

To probe the specificity of this interaction, two additional oligonucleotides were employed. One is MUT DNA, which contains four base pair substitutions on the 3′ or CG-rich side of the oligonucleotide, three of which reside within the currently defined consensus sequence (cf. Figure 2). A

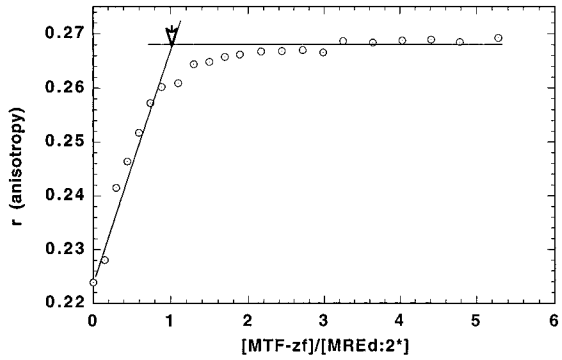

FIGURE 4: $Zn_{5.5}$-Cys_{12} MTF-zf binds to a coumarin-derivatized oligonucleotide duplex containing a single MREd binding site (MREd:2*; see Figure 2) and forms a 1:1 complex. This experiment also suggests that ≥90% of the protein in MTF-zf preparations is active in binding the MREd. Conditions: 7.8×10^{-8} M duplex, 40 mM MOPS, 0.20 M NaCl, pH 7.0, 25 °C.

promoter element containing four tandemly arranged MUT sequences has been previously shown to be largely inactive in metalloregulation in vivo, and fails to band-shift MTF-1 present in crude nuclear extracts (*2*). The other oligonucleotide is MT (*26*) which has been previously shown to possess a strong binding site for the general transcription factor Sp1; however, this 20-mer duplex contains just three nonconservative substitutions on the 5′ or TGCRC side of the site relative to MREd. Representative binding isotherms for coumarin-labeled MUT and MT DNAs are shown in Figure 5B and 5C, respectively. As can be seen, MUT binds MTF-zf ≈17-fold weaker than MREd:2* under the same solution conditions; this is consistent with the fact that the presence of 10-fold excess unlabeled MUT DNA in a MREd:2* binding reaction has essentially no effect on the returned K_{app} (data not shown). As expected, MTF-zf binds even weaker to MT DNA, $K_{app} = 5.8$ (± 2.3) $\times 10^6$ M^{-1}, or ≈60-fold weaker than MREd:2* DNA (Table 2). These findings suggest that MTF-zf binds with high affinity and specificity to a single MREd site and forms complexes of lower stability with non-native (MT) and nonfunctional MRE (MUT) sequences, in contrast to a previously published report (*3*).

Salt Dependence of the Binding of MTF-zf to the MREd. At moderate salt concentrations, examination of the salt-dependence of the K_{app} ($\partial \log K_{app}/\partial \log$ [NaX] or SK_{app}) can provide information on the stoichiometric participation of cations and anions in the binding reaction (*27*). Such a measurement can, in principle, provide an estimate of the extent to which electrostatic interactions stabilize the MTF-zf−MREd complex. The [NaCl] dependence of K_{app} is shown in Figure 6A for MREd:2* duplex. These data were derived from multiple "salt-back" titrations in which MTF-zf−MREd complexes formed at low salt are incrementally dissociated with the addition of small aliquots of a concentrated sodium chloride stock solution. A representative salt-back experiment shown in Figure 6B reveals that small changes in the concentration of sodium chloride greatly reduce the extent of complex formation; recovery of an anisotropy indistinguishable from that of the free DNA reveals that complex formation is reversible. Alternatively, binding isotherms were collected at various salt concentrations, and K_{app} was obtained directly. The slope of the plot of log K_{app} vs log [NaCl] is SK_{app}. Incorporating all of these

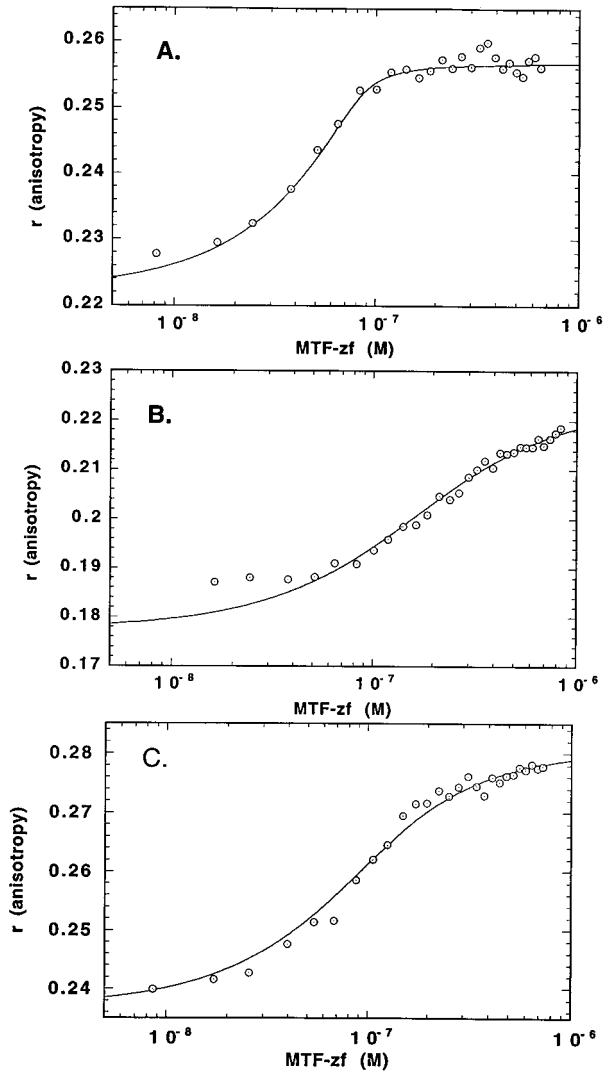

FIGURE 5: Fluorescence anisotropy titrations of MREd:2* (A), MT (B), and MUT (C) DNAs with $Zn_{5.5}$-Cys_{12} MTF-zf. Conditions: 7.8×10^{-8} M duplex, 40 mM MOPS, 0.20 M NaCl, pH 7.0, 25 °C. The nonlinear least-squares optimized values of K_{app} and $r_{complex}$ derived from a 1:1 binding model are for (A), $K_{app} = 3.98$ ($\pm$1.35) $\times 10^8$ M^{-1}; $r_o = 0.2224$; $r_{complex} = 0.2572$ ($\pm$0.0004); (B) $K_{app} = 7.78$ ($\pm$0.91) $\times 10^6$ M^{-1}; $r_o = 0.1775$; $r_{complex} = 0.2242$ ($\pm$0.0015); (C) $K_{app} = 2.21$ ($\pm$0.0.24) $\times 10^7$ M^{-1}; $r_o = 0.2367$; $r_{complex} = 0.2811$ ($\pm$0.0008).

data, SK_{app} for the MTF-zf−MREd:2* interaction is -11.0 ± 0.4.

A preliminary determination of the [NaF] dependence of MTF-zf−MREd:2* complex formation was also obtained. These results are shown in Figure 6A. F^- is considered a weakly interacting anion, compared to Cl^-; therefore, a significant reduction in the absolute magnitude of SK_{app} in F^--containing salts relative to Cl^--containing salts is indicative of the significant participation of anion release in the binding process. SK_{app} in NaF is -4.2 ± 0.5 (0.25−0.40 M NaF) or greater than 2-fold less negative than SK_{app} in NaCl. SK_{app} values in two divalent cationic salts, $MgCl_2$ and $ZnCl_2$, were also obtained (Table 3). As can be seen, SK_{app} is approximately −2 or about half that in NaF (see Discussion).

Temperature Dependence of the Stability of the MTF-zf−MREd:2 Complex*. A previous report suggested that the activation of binding of full-length MTF-1 to an MRE-containing oligonucleotide in crude extracts was a strong function of temperature (*3*). Investigation of the temperature dependence can also provide a determination of the thermodynamic driving force for complex formation over the physiological temperature range (*28*). The temperature dependence of K_{app} over the range extending from 5 to 37 °C was therefore determined for $Zn_{5.5}$ MTF-zf−MREd:2* complex formation at 0.30 M NaCl, pH 7.0. Representative isotherms are shown in Figure 7A with the temperature dependence of K_{app} plotted in the form of a van't Hoff plot (Figure 7B). As can be seen, the magnitude of K_{app} decreases at temperatures above and below ≈12 °C, resulting in a strongly nonlinear van't Hoff plot, suggesting that the nature of the thermodynamic driving force changes over the temperature range investigated. Nonlinear least-squares fitting of these data to a form of the Gibbs−Helmholtz equation allows extraction of $\Delta C°_{p,obs}$, the standard heat capacity change for complex formation; T_H, the temperature at which $\Delta H°_{obs} = 0$ and defines the temperature at which K_{app} is maximum, and T_S, the temperature at which $\Delta S°_{obs} = 0$, which defines the temperature at which $\Delta G°_{obs}$ is maximal (temperature of maximum stability). The solid curve through the experimental data in Figure 7B is defined by $\Delta C°_{p,obs} = -1.6 \pm 0.4$ kcal mol^{-1}; $T_H = 285 \pm 2$ K (12 $\pm$ 2 °C); $T_S = 291 \pm 2$ K (18 $\pm$ 2 °C).

*Effect of Zinc Occupancy of the Weak Binding Sites of MTF-zf on Modulating the Binding Affinity of MTF-zf to MREd:2**. The experiments above suggest that a subset of zinc fingers of MTF-zf bind zinc tightly and induce folding of these zinc fingers into a classical zinc finger fold.[2] Binding of zinc to the other weak-binding fingers has essentially no effect on the secondary structure of the molecule. It was therefore of interest to determine whether zinc occupancy of the weak-binding sites has any effect on the stability and energetics of complex formation. Representative isotherms are shown in Figure 8, in which isotherms obtained with $Zn_{5.5}$ MTF-zf, $Zn_{3.5}$ MTF-zf, and $Zn_{3.5}$ MTF-zf with Zn(II) added back at 0.20 M NaCl are compared; in addition, the binding affinity of partially oxidized MTF-zf was also investigated. K_{app} for some of these species was also obtained at 0.30 M NaCl, as was SK_{app}. The results of these experiments are summarized in Table 4. They show that there is a less than 4-fold reduction in K_{app} at 0.20 M and essentially no effect at 0.30 M NaCl when the fully reduced $Zn_{5.5}$ and $Zn_{3.5}$ forms of MTF-zf are compared, coupled with no significant effect on SK_{app}. Interestingly, partially oxidized $Zn_{5.5}$ MTF-zf binds to MREd:2* ≈30-fold weaker relative to the fully reduced species. These data suggest that the intrinsic binding affinity of MTF-zf to a single MRE sequence is not strongly modulated by zinc occupancy at the weak binding fingers, provided the Cys thiolates are in their reduced form.

DISCUSSION

Zn(II) and Cd(II) detoxification (*3*, *17*) and protection against oxidative stress (*29*, *30*) in vertebrate cells are mediated by the metal-dependent transcriptional activation of the expression of various metallothionein (MT) isoforms, which are collectively a conserved family of cysteine-rich

[2] The true affinity of the tight zinc-binding sites in MTF-zf for zinc cannot be directly measured since removal of zinc from these sites results in precipitation of the protein.

Table 2: Summary of DNA-Binding Parameters of $Zn_{5.5}$ MTF-zf to Various Coumarin-Derivatized Oligonucleotides As Determined by Fluorescence Anisotropy Titrations[a]

oligonucleotide	[NaCl] (M)	K_{app} (M^{-1})[b]	r_o	Δr
MREd:2*	0.20	3.8 (±0.5) × 10^8 ($n = 4$)	0.227 (±0.016)	0.036 (±0.005)
	0.30	1.3 (±0.2) × 10^7 ($n = 5$)		
MREd:1*	0.20	3.7 (±0.2) × 10^8 ($n = 2$)	0.232 (±0.017)	0.011 (±0.002)
	0.30	1.6 (±0.2) × 10^7		
MUT	0.20	2.2 (±0.3) × 10^7	0.236 (±0.001)	0.044
MT	0.20	5.8 (±2.3) × 10^6 ($n = 3$)	0.196 (±0.016)	0.035 (±0.010)

[a] 40 mM MOPS at the indicated [NaCl], pH 7.0, 25 °C. [b] Number of independent titrations (n) indicated in parentheses.

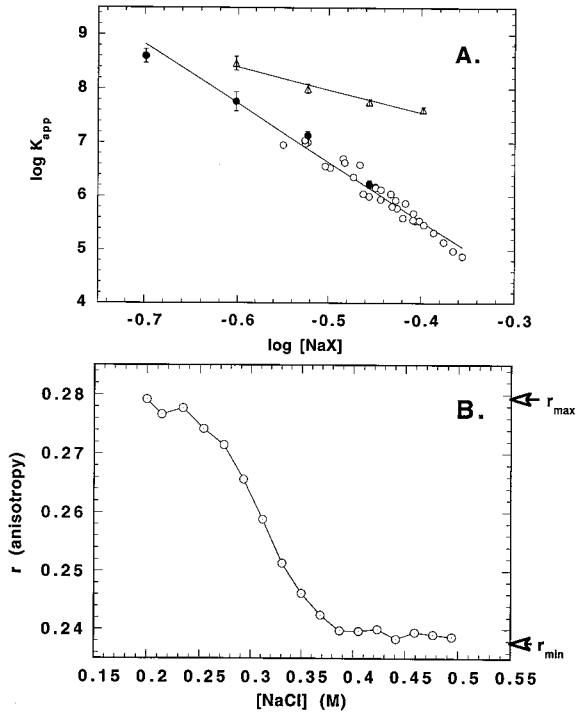

FIGURE 6: (A) log K_{app}−log [NaX] plots of the effect of [NaCl] (○, ●) or [NaF] (△) on the binding affinity of MTF-zf to MREd:2* obtained from a simultaneous analysis of saltback titrations such as those shown in panel B (*45*) as well as from individual titrations obtained at various [NaX] (●, △). The $\partial \log K_{app}/\partial \log$ [NaX] (SK_{app}) values for the MREd:2* oligonucleotide in NaCl and NaF are −11.0 (±0.4) and −4.2 (±0.5), respectively. (B) Representative [NaCl]-induced salt-back titration of the MTF-zf−MREd:2* complex formed at 0.20 M NaCl.

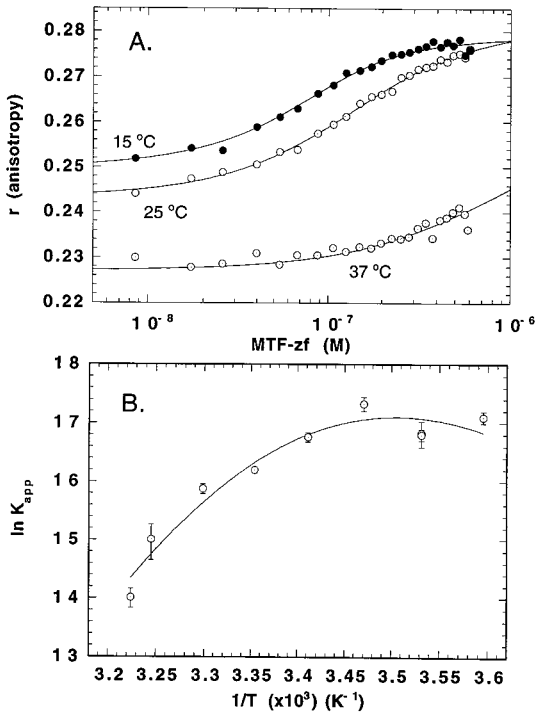

FIGURE 7: Temperature dependence of the binding of MTF-zf to MREd:2*. Conditions: 7.8 × 10^{-8} M DNA, 40 mM MOPS, 0.30 M NaCl, pH 7.0, at the indicated temperature. (A) Representative individual fluorescence anisotropy isotherms collected at 15 °C [K_{app} = 3.35 (±0.40) × 10^7 M^{-1}; r_o = 0.2496; $r_{complex}$ = 0.2790 (±0.0005)], 25 °C [K_{app} = 1.08 (±0.06) × 10^7 M^{-1}; r_o = 0.2432; $r_{complex}$ = 0.2814 (±0.0006)], and 37 °C [K_{app} = 1.1 (±0.3) × 10^6 M^{-1}; r_o = 0.2271; $r_{complex}$ = 0.263 (±0.003)]. (B) van't Hoff plot of the effect of temperature on the binding of MTF-zf to MREd:2* over the range 5−37 °C. The solid curve is a nonlinear least-squares fit to the relationship $\ln K_{obs} = (\Delta C°_{p,obs}/R)[(T_H/T) - 1 - \ln(T_s/T)]$ with resolved parameters $\Delta C°_{p,obs}$ = −1.6 ± 0.4 kcal mol^{-1}, T_H = 285 ± 2 K (12 ± 2 °C), T_S = 291 ± 2 K (18 ± 2 °C). T_H is the temperature at which K_{app} is maximal; T_S is the temperature of maximum stability.

Table 3: Salt Dependence of the Binding of Various MTF-zf Preparations to MREd:2* As Determined by Fluorescence Anisotropy Titrations[a]

MTF-zf preparation	salt type	[salt] range	SK_{app}
$Zn_{5.5}$ Cys_{12}	NaCl	0.20−0.44 M	−11.0 (±0.4)
	NaF	0.25−0.40 M	−4.2 (±0.5)
	$ZnCl_2$	0.3−0.7 mM	−2.1 (±0.2)
	$MgCl_2$	2.5−13.6 mM	−1.6 (±0.2)
$Zn_{3.5}$ Cys_{12}	NaCl	0.28−0.39 M	−9.6 (±1.0)
$Zn_{3.5}$ Cys_{12} + Zn(II)[b]	NaCl	0.28−0.36 M	−9.6 (±1.4)
$Zn_{(3)}$ Cys_6 MTF-zf	NaCl	0.23−0.35 M	−10.7 (±1.3)

[a] 40 mM MOPS in the presence of the indicated salt, pH 7.0, 25 °C. [b] 3 molar equiv of Zn(II) relative to MTF-zf.

transition metal-binding proteins. Although the molecular mechanism by which MTs mediate these responses and maintain metal ion homeostasis is not yet clear, cis-acting metal-response elements (MREs) found in the promoter regions of all MT genes are required for the metal-induced transcriptional activation (*12*). Further, MTF-1 is the protein factor which is essential for activation of MT expression mediated through the MREs (*2*, *13*, *14*).

To obtain molecular insight into plausible mechanisms by which human MTF-1 mediates metal detoxification, the structure and energetics of the binding of highly purified MTF-1 or domain fragments to oligonucleotide duplexes under well-defined solution conditions must be obtained. Here, we report that the zinc finger domain (MTF-zf) of MTF-1 binds with high affinity and specificity to a 23-mer oligonucleotide containing a single consensus MREd sequence forming a 1:1 complex. Zn(II) MTF-zf binds the MREd with a large [NaCl] dependence. Although additional studies are clearly required, interpretation of the salt dependence of MTF-zf−MREd complex formation according to

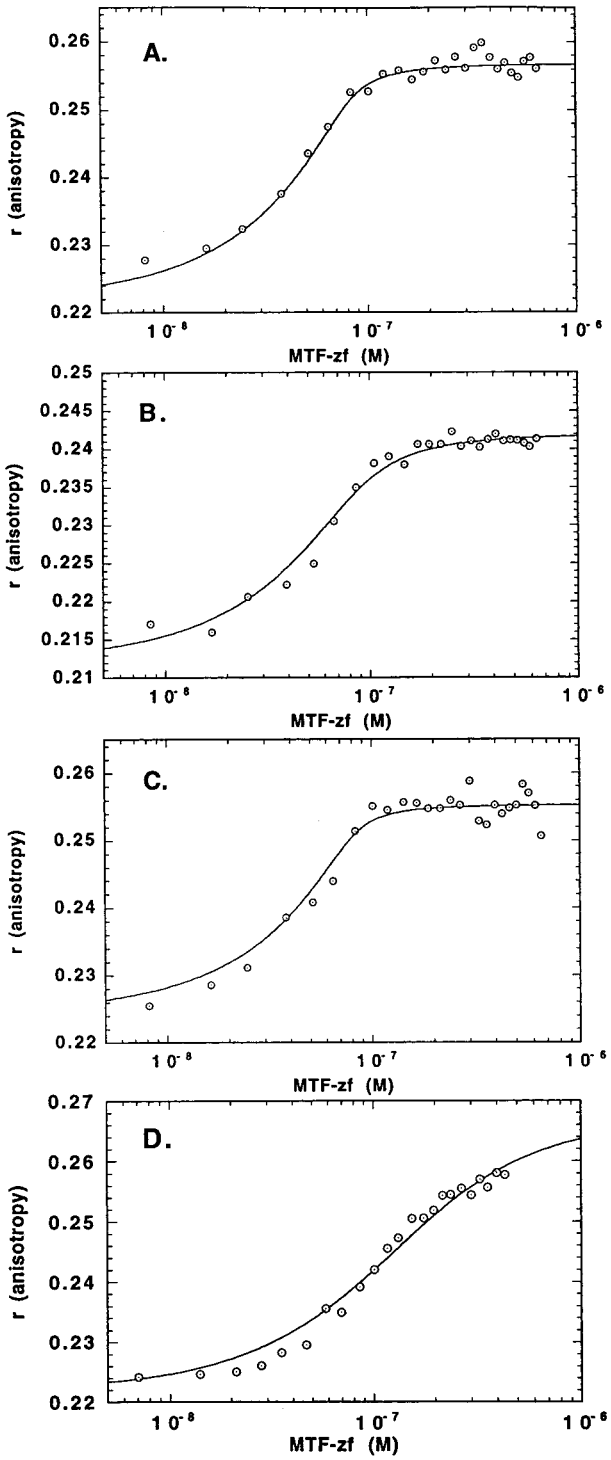

FIGURE 8: Zn(II) binding to the weak Zn(II) sites in MTF-zf has little or no effect on the affinity of the MTF-zf−MREd:2* complex. The solution conditions are 40 mM MOPS, 0.20 NaCl, pH 7.0, 25 °C. $Zn_{3.5}$-Cys_{12} MTF-zf was prepared from $Zn_{5.5}$-Cys_{12} MTF-zf by incubation with 4.5 molar equiv of mag-fura-2 followed by exhaustive dialysis against metal-free buffer (see Table 1). Average binding parameters are summarized in Table 4. (A) $Zn_{5.5}$-Cys_{12} MTF-zf: $K_{app} = 3.98\ (\pm 1.35) \times 10^8\ M^{-1}$; $r_o = 0.2224$; $r_{complex} = 0.2572\ (\pm 0.0004)$. (B) $Zn_{3.5}$-Cys_{12} MTF-zf: $K_{app} = 1.15\ (\pm 0.26) \times 10^8\ M^{-1}$; $r_o = 0.2123$; $r_{complex} = 0.2420\ (\pm 0.0004)$. (C) $Zn_{3.5}$-Cys_{12} MTF-zf plus 3 molar equiv of Zn(II): $K_{app} = 4.49\ (\pm 2.90) \times 10^8\ M^{-1}$; $r_o = 0.2245$; $r_{complex} = 0.2553\ (\pm 0.0006)$. (D) Partially oxidized $Zn_{(3)}$-Cys_6 MTF-zf: $K_{app} = 1.18\ (\pm 0.21) \times 10^7\ M^{-1}$; $r_o = 0.2202$; $r_{complex} = 0.2675\ (\pm 0.0023)$.

standard polyelectrolyte theory (*31*) suggests that as many as ≈4 net Na^+ ions or ≈2 divalent cations [in Zn(II)- or Mg(II)-containing buffer salts] and up to 6−7 Cl^- ions from MTF-zf may be released into bulk solution upon complex formation. If all of the Na^+ ions are released from the DNA duplex, as many as five electrostatic interactions may characterize the complex, a value not unreasonable from examination of the structures of other Cys_2-His_2 zinc finger−DNA complexes (*32*, *33*). Consistent with findings for other sequence-specific and nonspecific protein−DNA interactions, the absolute value of K_{app} in NaF is significantly larger than that in NaCl at the same [NaX] over the entire range of [NaX] examined (0.25−0.45 M) (*31*, *34*, *35*). Although part of this difference lies in the distinct SK_{app} obtained in NaCl vs NaF, it cannot account for all of it. F^- ions relative to Cl^- ions are thought to preferentially hydrate protein surfaces; this may enhance the stability of the complex. In addition, examination of the temperature dependence of Zn(II) MTF-zf−MREd complex formation reveals that the binding process is accompanied by a large negative standard heat capacity change. Unfortunately, the salt and temperature dependencies of the specific DNA binding by other zinc finger proteins have not yet been reported; therefore, comparisons with other related systems cannot yet be made. However, the vast majority of site-specific protein−DNA interaction systems which have been investigated appear to be characterized by a large negative standard heat capacity change comparable to the magnitude reported here for the MTF-zf−MREd:2* interaction (*36*). Although the molecular origin of this large negative $\Delta C^\circ_{p,obs}$ is under discussion (*37*, *38*), some or all of this may reflect burial of nonpolar surface area or induced polypeptide folding which accompanies complex formation (*36*).

As MTF-1 is a Cys_2-His_2 zinc finger protein, this has led to speculation that MTF-1, and, in particular, the zinc finger domain of MTF-1, may function as both a sensor of free zinc concentration and a transducer of the biological response (activation of MT expression). Andrews and co-workers have presented evidence in support of this scenario (*3*, *17*); however, other experiments, which tested the ability of MTF-zf−VP16 or GAL4−MTF-1 chimeric proteins to regulate the expression of a reporter gene in a heterologous expression system in a zinc-dependent manner in vivo, proved to be less conclusive (*16*). One possible explanation is that full-length MTF-1 is required to effect Zn(II)-dependent modulation of MRE-binding affinity, through either an intramolecular (*17*) or an intermolecular (*39*) mechanism. Indeed, the acidic and proline-rich activation domains immediately C-terminal to the zinc finger domain (Figure 1A) appear to play some role in Zn(II) regulation but only in the context of intact MTF-1, consistent with a structurally ill-defined "complex interplay" among various functional domains of the molecule (*16*).

Although the studies reported here do not directly address a metalloregulatory role played by the zinc finger domain itself, our characterization of MTF-zf places limitations on what metolloregulatory models are plausible. For example, we find that the isolated MTF-1 zinc finger domain has at least two classes of zinc-binding sites, a picture potentially consistent with a mixture of structural and metalloregulatory zinc sites in the molecule. Zinc occupancy of three or so tight-binding sites in MTF-zf induces sufficient secondary structure in the molecule to fold at least three zinc finger sequences into the classical $\beta\beta\alpha$ fold. These "structural"

Table 4: Effect of Zinc Composition and Cysteine Oxidation State of MTF-zf on the MREd:2*-Binding Properties of MTF-zf As Determined by Fluorescence Anisotropy Titrations[a]

MTF-zf preparation	[NaCl] (M)	K_{app} (M^{-1})[b]	r_o	Δr
$Zn_{5.5}$ Cys_{12}	0.20	3.8 (±0.5) × 10^8 ($n = 4$)	0.227 (±0.016)	0.036 (±0.005)
	0.30	1.3 (±0.2) × 10^7 ($n = 5$)		
$Zn_{3.5}$ Cys_{12}	0.20	1.1 (±0.2) × 10^8	0.208 (±0.008)	0.024 (±0.005)
	0.30	1.4 (±0.2) × 10^7		
$Zn_{3.5}$ Cys_{12} + Zn(II)[c]	0.20	4.5 (±1.3) × 10^8	0.225	0.044
$Zn_{(3)}$ Cys_6	0.20	1.2 (±0.2) × 10^7	0.222	0.045

[a] 40 mM MOPS at the indicated [NaCl], pH 7.0, 25 °C. [b] Number of independent titrations (n) indicated in parentheses. [c] 3 molar equiv of Zn(II) relative to MTF-zf.

sites are necessary and sufficient for high-affinity MREd binding. These findings further make it unlikely that metal-free MTF-1 would stably exist inside cells, consistent with a constitutively expressed Zn_3 MTF-1 bound to the MRE in such a way that both basal and zinc-activated transcription from the MT promoter might be effected, as previously found (*14*).

In contrast, binding of Zn(II) to the "weak" sites in MTF-zf appears to have no effect on the structure of the protein or the efficacy of MREd binding, findings unanticipated on the basis of previous results (*3*, *17*). The function of these weak sites in MTF-1 is unclear. If they do play a metalloregulatory role by functioning as a zinc sensor or transducer, metalloregulation must occur at some other level beyond modulation of DNA-binding affinity to a single MREd, e.g., in transcriptional activation itself. Alternatively, detection of a metalloregulatory role played by these sites may simply require intact MTF-1 or amino acid sequences outside of the zinc finger domain. What is clear is that classical zinc finger folding does not readily occur in two to three of the Cys_2-His_2 sequence motifs within MTF-zf, even in the presence of high (2 mM) Zn(II). Any further structural features of these zinc coordination complexes are not yet known. For example, weak Zn(II) binding to these sites may be an intrinsic feature of each of these zinc finger sequence motifs; alternatively, there may be strong negative cooperativity of zinc binding operating within the MTF-zf domain. There are at least two examples of isolated Cys_2-His_2 sequence domains which fail to bind Zn(II) in vitro; these have been shown to occur in an N-terminal finger of a multi-finger protein (*40*, *41*). Further, we note that there are at least several examples of Cys_2-His_2 zinc finger proteins which appear to utilize only a subset of their zinc fingers to interact specifically with their specific DNA targets (*42*), or, in the case of TFIIIA, provide much of the DNA-binding energy (*43*, *44*). Thus, MTF-zf may not be unusual in this regard.

Once the structural zinc fingers of MTF-1 have been identified, "broken finger" and "missing finger" mutants of MTF-zf as well as intact MTF-1 will be characterized to further define the regulatory properties of MTF-1, to be aided by more extensive characterization of the metal-binding and MRE-binding properties of single-finger peptide domains of the molecule. It is interesting to note that Zap1p, a metalloregulatory protein integral to mediating zinc-responsive transcriptional regulation in *S. cerevisiae* under zinc-limiting conditions, contains 5 putative Cys_2-His_2 zinc fingers (a 6th one is missing just 1 of the 4 zinc ligands) at the C-terminus of an 880 amino acid molecule (*5*). This domain is appended to a large N-terminal domain containing 12% Cys and His residues, some of which are clustered; a single metalloregulatory point mutant has been isolated in the N-terminal domain coincident with one of the transcriptional activation domains (*5*). Although MTF-1 contains no such Cys-His-rich domain, further studies are required to determine the extent to which regulatory mechanisms are similar or different in MTF-1 vs Zap1p.

ACKNOWLEDGMENT

We thank Dr. Raza Khan for construction and sequencing of the bacterial MTF-zf expression plasmid, as well as Dr. Walter Schaffner, University of Zürich, for providing the pChMTF-1 plasmid.

REFERENCES

1. O'Halloran, T. V. (1993) *Science 261*, 715−725.
2. Radtke, F., Heuchel, R., Georgiev, O., Hergersberg, M., Gariglio, M., Dembic, Z., and Schaffner, W. (1993) *EMBO J. 12*, 1355−1362.
3. Dalton, T. P., Bittel, D., and Andrews, G. K. (1997) *Mol. Cell. Biol. 17*, 2781−2789.
4. Erbe, J. L., Taylor, K. B., and Hall, L. M. (1995) *Nucleic Acids Res. 23*, 2472−2478.
5. Zhao, H., and Eide, D. J. (1997) *Mol. Cell. Biol. 17*, 5044−5052.
6. Berg, J. M., and Shi, Y. (1996) *Science 271*, 1081−1085.
7. Stuart, G. W., Searle, P. F., and Palmiter, R. D. (1985) *Nature 317*, 828−831.
8. Karin, M., Haslinger, A., Holtgreve, H., Richards, R. I., Krauter, P., Westpahl, H. M., and Beato, M. (1984) *Nature 308*, 513−519.
9. Kägi, J. H. R., and Schäffer, A. (1988) *Biochemistry 27*, 8509−8515.
10. Michalska, A. E., and Choo, K. H. A. (1993) *Proc. Natl. Acad. Sci. U.S.A. 90*, 8088−8092.
11. Masters, B. A., Kelly, E. J., Quaife, C. J., Brinster, R. L., and Palmiter, R. D. (1994) *Proc. Natl. Acad. Sci. U.S.A. 91*, 584−588.
12. Stuart, G. W., Searle, P. F., Chen, H. Y., Brinster, R. L., and Palmiter, R. D. (1984) *Proc. Natl. Acad. Sci. U.S.A. 81*, 7318−7322.
13. Brugnera, E., Georgiev, O., Radtke, F., Heuchel, R., Baker, E., Sutherland, G. R., and Schaffner, W. (1994) *Nucleic Acids Res. 22*, 3167−3173.
14. Heuchel, R., Radtke, F., Georgiev, O., Stark, G., Aguet, M., and Schaffner, W. (1994) *EMBO J. 13*, 2870−2875.
15. Westin, G., and Schaffner, W. (1988) *EMBO J. 7*, 3763−3770.
16. Radtke, F., Georgiev, O., Müller, H.-P., Brugnera, E., and Schaffner, W. (1995) *Nucleic Acids Res. 23*, 2277−2286.
17. Bittel, D., Dalton, T., Samson, S. L.-A., Gedamu, L., and Andrews, G. K. (1998) *J. Biol. Chem. 273*, 7127−7133.
18. Párraga, G., Horvath, S. J., Eisen, A., Taylor, W. E., Hood, L., Young, E. T., and Klevit, R. E. (1988) *Science 241*, 1489−1492.
19. Fürst, P., Hu, S., Hackett, R., and Hamer, D. (1988) *Cell 55*, 705−717.

20. Studier, F. W., Rosenberg, A. H., Dunn, J. J., and Dubendorff, J. W. (1990) *Methods Enzymol. 185*, 60−89.
21. Guo, J., and Giedroc, D. P. (1997) *Biochemistry 36*, 730−742.
22. Heyduk, T., and Lee, J. C. (1990) *Proc. Natl. Acad. Sci. U.S.A. 87*, 1744−1748.
23. Giedroc, D. P., Khan, R., and Barnhart, K. (1991) *Biochemistry 30*, 8230−8242.
24. Walkup, G. K., and Imperiali, B. (1997) *J. Am. Chem. Soc. 119*, 3443−3450.
25. Qiu, H., Kodadek, T., and Giedroc, D. P. (1994) *J. Biol. Chem. 269*, 2773−2781.
26. Kriwacki, R. W., Schultz, S. C., Steitz, T. A., and Caradonna, J. P. (1992) *Proc. Natl. Acad. Sci. U.S.A. 89*, 9759−9763.
27. Record, T., Jr., Ha, J.-H., and Fisher, M. A. (1991) *Methods Enzymol. 208*, 292−343.
28. Ha, J.-H., Spolar, R. S., and Record, M. T., Jr. (1989) *J. Mol. Biol. 209*, 801−816.
29. Dalton, T. P., Li, Q., Bittel, D., Liang, L., and Andrews, G. K. (1996) *J. Biol. Chem. 271*, 25233−25241.
30. Dalton, T., Palmiter, R. D., and Andrews, G. K. (1994) *Nucleic Acids Res.*, 5016−5023.
31. Ha, J.-H., Capp, M. W., Hohenwalter, M. D., Baskerville, M., and Record, M. T., Jr. (1992) *J. Mol. Biol. 228*, 252−264.
32. Foster, M. P., Wuttke, D. S., Radhakrishnan, I., Case, D. A., Gottesfeld, J. M., and Wright, P. E. (1997) *Nat. Struct. Biol. 4*, 605−608.
33. Kim, C. A., and Berg, J. M. (1996) *Nat. Struct. Biol. 3*, 940−945.
34. Overman, L. B., and Lohman, T. M. (1994) *J. Mol. Biol. 236*, 165−178.
35. Villemain, J. L., and Giedroc, D. P. (1996) *J. Biol. Chem. 271*, 27623−27629.
36. Spolar, R. S., and Record, M. T., Jr. (1994) *Science 263*, 777−784.
37. Ferrari, M. E., and Lohman, T. M. (1994) *Biochemistry 33*, 12896−12910.
38. Lohman, T. M., Overman, L. B., Ferrari, M. E., and Kozlov, A. G. (1996) *Biochemistry 35*, 5272−5279.
39. Palmiter, R. D., Cole, T. B., Quaife, C. J., and Findley, S. D. (1996) *Proc. Natl. Acad. Sci. U.S.A. 93*, 14934−14939.
40. Neuhaus, D., Nakaseko, Y., Schwabe, J. W. R., and Klug, A. (1992) *J. Mol. Biol. 228*, 637−651.
41. Fairall, L., Schwabe, J. W. R., Chapman, L., Finch, J. T., and Rhodes, D. (1993) *Nature 366*, 483−487.
42. Pavletich, N. P., and Pabo, C. O. (1993) *Science 261*, 1701−1707.
43. Clemens, K. R., Zhang, P., Liao, X., McBryant, S. J., Wright, P. E., and Gottesfeld, J. M. (1994) *J. Mol. Biol. 244*, 23−35.
44. Del Rio, S., and Setzer, D. R. (1993) *Proc. Natl. Acad. Sci. U.S.A. 90*, 168−172.
45. Overman, L. B., Bujalowski, W., and Lohman, T. M. (1988) *Biochemistry 27*, 456−471.

BI980843R